HHS Public Access

Author manuscript

Small. Author manuscript; available in PMC 2016 April 01.

Published in final edited form as:

Small. 2015 April ; 11(13): 1519–1525. doi:10.1002/smll.201402369.

Biodegradable Nanoellipsoidal Artificial Antigen Presenting Cells for Antigen Specific T-Cell Activation

Randall A. Meyer,
Translational Tissue Engineering Center, Institute for Nanobiotechnology, Department of Biomedical Engineering, Johns Hopkins School of Medicine, 400 N Broadway, Baltimore MD, 21231, USA

Joel C. Sunshine,
Translational Tissue Engineering Center, Institute for Nanobiotechnology, Department of Biomedical Engineering, Johns Hopkins School of Medicine, 400 N Broadway, Baltimore MD, 21231, USA

Karlo Perica,
Institute for Cell Engineering, Department of Pathology, Johns Hopkins School of Medicine, 733 N Broadway, Baltimore MD, 21205, USA

Alyssa K. Kosmides,
Institute for Cell Engineering, Department of Pathology, Johns Hopkins School of Medicine, 733 N Broadway, Baltimore MD, 21205, USA

Kent Aje,
Institute for Cell Engineering, Department of Pathology, Johns Hopkins School of Medicine, 733 N Broadway, Baltimore MD, 21205, USA

Jonathan P. Schneck [Prof.], and
Institute for Cell Engineering, Department of Pathology, Johns Hopkins School of Medicine, 733 N Broadway, Baltimore MD, 21205, USA

Jordan J. Green [Prof.]
Translational Tissue Engineering Center, Institute for Nanobiotechnology, Department of Biomedical Engineering, Johns Hopkins School of Medicine, 400 N Broadway, Baltimore MD, 21231, USA

Jordan J. Green: green@jhu.edu

Keywords

Nanoparticles; Immunoengineering; CD8+ T-Cell activation; Particle shape; Biomimetic

Correspondence to: Jordan J. Green, green@jhu.edu.

RM and JCS contributed equally to this work.

Supporting Information

Supporting Information is available from the Wiley Online Library or from the author.

Biomimetic artificial antigen presenting cells (aAPCs) have shown substantial promise as a platform for immune system activation and modulation. Antigen specific aAPCs reconstitute the critical T-Cell recognition ("signal 1") and activation ("signal 2") signals presented at the surface of APCs by presenting peptide-in-MHC and positive costimulatory molecules such as anti-CD28 antibody on the surface of the particle. Classically, aAPCs are cell sized (2–10 μm), spherical particles, and have been made using a variety of materials, from liposomes[1, 2] to magnetic beads,[3–7] to non-degradable[8] and degradable polymeric microparticles.[9–11] Despite the extensive *in vitro* data supporting the efficacy of these particles *in vitro*, *in vivo* translation has been limited due to the poor bioavailability and activity of spherical micron sized particles. Nanoparticle systems offer an attractive alternative to micron sized particles as drug delivery vehicles for the aAPC platform. Recently, nanoparticles have been utilized for various therapeutic and diagnostic applications, such as tumor targeting and imaging.[12–16] Biodistribution of these drug carriers has been of special interest in the past few years, as efforts have been made to engineer nanoparticles that simultaneously target the region of interest and can be eliminated efficiently to avoid toxicity.[17–20]

One major issue with attempting to translate the aAPC technology onto the nanoscale is that the literature strongly supports the concept that receptor occupancy over a large surface area of contact is a critical determinant for activation; for aAPCs, 4–5 μm particles were found to be superior to 1 μm particles, and the difference could not be made up simply by increasing the particle dose.[8] However, these systems use spherical particles as the core of the construct which, for a given volume, provide the minimum surface area of contact between a T-Cell and aAPC.

Non-spherical, anisotropic nanoparticles have recently gained increasing attention within the biomaterials community for a numerous reasons. A wide variety of shapes have been synthesized by bottom-up and top-down approaches.[21, 22] Nanoparticles with altered shape offer potential improvements in intracellular particle delivery and *in vivo* circulation time by aligning with blood flow and reducing phagocytosis,[23, 24] enhanced targeting of diseased microvasculature,[25] reduction of non-specific particle uptake,[26] and improved specific particle uptake and cancer cell killing.[27] In particular, prolate ellipsoids (semi-axes: a>b=c) showed the most efficient particle attachment with lowest *in vitro* internalization rates when compared to oblate ellipsoids (semi-axes: a=b>c) or spherical particles.[28] Non-spherical prolate nanoellipsoids have shown enhanced tissue targeting of brain and lung endothelium.[29] With regard to immune stimulation, we have recently shown that non-spherical microparticles were much more successful at functioning as aAPCs compared to spherical microparticle aAPCs, inducing stronger, and more efficient, antigen specific T-Cell responses.[30]

For nanoscale aAPCs (naAPCs), altering the particle shape could allow for an interfacial geometry (at the interface between the aAPC and the T-Cell) that is more similar to successful microparticulate systems, including a microscale radius of curvature for the long axis. In addition, non-spherical naAPCs have the potential for improved *in vivo* biodistribution as compared to microparticles due to easy access to draining lymph nodes and suitability for intravenous injection. Non-spherical naAPCs can also take advantage of a

shape-dependent reduction in non-specific uptake and improved circulation time through avoidance of the RES system. Based upon these proposed benefits, we elected to study how shape might affect naAPC function and *in vivo* biodistribution. In addition, while aAPCs are often constructed of nondegradable materials for *ex vivo* use, we wished to construct effective biodegradable nanoscale aAPCs for the first time to make them more amenable for *in vivo* therapeutic use.

To study the utility of non-spherical naAPCs for antigen-specific T-cell activation, we adapted a film stretching technique originally developed by Ho et al[31] and more recently adapted to generate polymeric micro- and nanoparticles of varied shape.[32] To ensure biodegradability of the naAPCs, we synthesized PLGA nanoparticles using a single-emulsion with sonication method (see supplemental methods for details). We then cast them in a thin PVA film, and either stretched the film at 90°C or not (to fabricate ellipsoid or spheroid particles respectively), and then removed the nanoparticles by dissolution (Figure 1a). We applied different amounts of stretch extent to the film to generate a range of nanoparticle aspect ratios. Generation of prolate ellipsoids from spherical nanoparticles yields high aspect ratio and large radius of curvature particles with minimal change to overall particle surface area (see Table S1 and ref 30 for more details). For example, a 2-fold stretch of a 200 nm spherical particle produces a prolate ellipsoid with an aspect ratio of 2.8, a radius of curvature along the long axis of 1.14 μm, and a modest surface area gain of 16%. Thus with an ellipsoidal aAPC, we can mimic the more effective microparticle based aAPC radius of curvature. We then fabricated the spherical and ellipsoidal nanoparticles into aAPCs by adding peptide loaded MHC-IgG dimers (pMHC-dimers) and anti-CD28 mAb to their surface via EDC/NHS chemistry to conjugate to the acid terminated PLGA polymer (Figure 1a).

The generated PLGA nanoparticles were 225 nm in diameter with a slightly net negative charge (−2.9±0.8 mV in PBS); stretching the particles resulted in ellipsoidal nanoparticles with the same volume that were also similarly slightly negatively charged (−2.2±0.2 mV in PBS). Stretching was confirmed by TEM analysis utilizing a negative stain of 1% uranyl acetate (Figure 1b-e). We conjugated fluorophore-labeled MHC-IgG dimer (labeled with Alexa 488) and labeled anti-CD28 mAb (labeled with APC) to the surface of spherical and ellipsoidal nanoparticles and quantified the total fluorescence on the particles by plate reader. Spherical and ellipsoidal nanoparticles showed similar levels of MHC-IgG dimer and anti-CD28 mAb conjugation. In addition, increasing amounts of MHC-IgG dimer and anti-CD28 in synthesis lead to an increased amount of protein conjugated to the particle surface, indicating that aAPC synthesis was concentration dependent over the range tested (Figure 1 f-g). We also examined particle stability by conjugating fluorescently-labeled MHC-IgG dimer and anti-CD28 to the surface of the particles, incubating the particles in physiological conditions (1x PBS at 37 °C), and analyzing particle stability at various points in time. As shown, the spherical particles and ellipsoidal particles exhibited similar stability *in vitro* and more than 50% of the proteins were still conjugated to particles after incubation for 7 days (Figure S1).

To examine whether these functionalized naAPCs could generate antigen specific CD8+ T-Cell responses, we coupled gp100-loaded MHC-Ig dimer (or non-cognate peptide loaded

dimer) and anti-CD28 monoclonal antibody (mAb) to the surface of spherical and ellipsoidal nanoparticles. Since optimal particle dosing was unknown, and particle/antigen dose has been previously shown to be a critical parameter in activation of T-Cells by other aAPC systems, we performed a dose titration. T-Cells were exposed *in vitro* to 1 mg, 0.1 mg, and 0.01 mg PLGA naAPC / 100,000 cells, and antigen specific T-Cell expansion was evaluated via CFSE dilution (3 days post stimulation) and total T-Cell proliferation (7 days post stimulation).

CFSE dilution analysis of the non-spherical 2-fold stretched naAPCs vs. the spherical naAPCs revealed a clear shape dependency on initial proliferation rates (Figure 2a-c). This effect was noted to be most profound at the middle dose of 0.1 mg/100,000 T-Cells (Figure 2b). The lowest dose of 0.01 mg/100,000 cells appeared to have little effect on T-Cell proliferation for either spherical or nonspherical aAPC (Figure 2a). At the highest dose of 1 mg / 100,000 cells both spherical and non-spherical naAPCs were effective at stimulating T-Cells (Figure 2c). Based on these results we decided to probe the effect of shape further by analyzing the effect of different degrees of stretch (1.5, 2, 2.5, 3, 3.5-fold) on the naAPC activation of CD8+ T-Cells. Generation analysis of CFSE data revealed that naAPCs were not effective at the low dose of 0.01 mg/100,000 T-Cells (Figure 2d). In addition, all naAPC formulations were able to generate > 10-fold antigen-specific T-Cell proliferation at a saturating dose of 1 mg/100,000 T-Cells (Figure 2f). However, at the mid-range dose of 0.1 mg / 100,000 cells, there was a marked difference at aAPC stimulation of the spherical and non-spherical naAPCs (Figure 2e).

T-Cell proliferation counts reflected the trends demonstrated in the CFSE generation data. At the lowest dose of naAPC stimulation (Figure 2g), there was little stimulation of all particle shapes tested except for 2.5-fold stretched naAPC, which demonstrated a significant ($p < 0.05$) increase in proliferation (3-fold) compared to spherical naAPC (1-fold). The clearest shape dependency was demonstrated at the mid-range dose (Figure 2h). All ellipsoidal naAPC significantly outperformed the spherical naAPC ($p < 0.05$). As an example, the 2-fold stretched naAPC induced a 15-fold expansion of the T-Cells compared to the spherical particles which induced a 3-fold expansion. The benefit of the non-spherical shape was apparent at the high dose (Figure 2i), and significant ($p <0.05$) for the 2.5-fold and 3.5-fold stretched naAPC. To simplify experimental comparison, all subsequent studies in this work were conducted with the spherical and the 2-fold stretched ellipsoidal particles.

In addition to offering a functional benefit to T-Cell stimulation, another potential advantage of ellipsoidal naAPC is that they may offer improved *in vivo* drug delivery properties, such as a reduction in non-specific cell uptake.[28] To that end, we investigated whether nanoparticle uptake was shape dependent. By loading PLGA nanoparticles with a fluorescent dye (TAMRA), we were able to examine the impact of particle shape on uptake by confocal microscopy and flow cytometry. We modeled two different modes of uptake. For phagocytic cells present in the reticuloendothelial system (RES), RAW 264.7 macrophages were used as a model. Confocal analysis of the macrophages treated with 0.1 mg of particles / 15,000 cells demonstrated a clear preference for spherical particles (Figure 3a) vs. non-spherical particles (Figure 3b). Flow cytometry analysis reflected this difference across a variety of doses (Figure 3c) and incubation times (Figure 3e). Maximal dose-

dependent uptake was determined to be 78% for the spherical particles and 14% for the ellipsoidal particles. Over the course of 72 hours, the uptake percentages equilibrated between the spherical and ellipsoidal groups demonstrating the capability of the ellipsoidal particles to resist uptake.

As a model of non-specific uptake by endocytosis in vascular cells, we looked at particle uptake in primary human umbilical vein endothelial (HUVEC) cells *in vitro*. Spherical particles were taken up by up to 10% of the HUVEC cells during a 24 hour incubation period, with increasing frequency given an increased particle concentration (Figure 3d). In addition, the amount of particles taken up by the cells was noted to increase over longer incubation times (Figure 3f). We saw no significant ellipsoidal particle uptake at any particle dose or at any time point in the HUVECs. Representative gated flow cytometry plots show spherical particle uptake for the HUVECs and macrophages (Figure S2). Viability of RAW macrophages was similar between the spherical and nonspherical particle groups at all doses (Figure S3).

Next, we sought to validate the *in vitro* shape dependent uptake seen with HUVECs and macrophages *in vivo* by performing a biodistribution experiment to evaluate the circulation half-life and overall distribution characteristics of the ellipsodial naAPCs compared to the spherical naAPCs. Biodistribution of spherical and ellipsoidal naAPCs were examined in nude SCID mice over a four-hour period. naAPCs for biodistribution were synthesized encapsulating a custom made hydrophobic 800nm near IR dye (LI-COR Bioservices) in the interior of the naAPCs and conjugating MHC-IgG dimer and mouse anti-CD28 mAb to the naAPC surface. Two groups of nude mice received 100,000 fluorescent units of spherical or ellipsoidal naAPC via tail vein injections. Retroorbital bleeding was conducted at 10, 20, 30 and 40 minute intervals after injections of naAPC to determine blood clearance. Mice were then imaged with a LI-COR Pearl Impulse at 1, 2 and 4 hours post injection to evaluate biodistribution. After the 4 hour time point of imaging, mice were sacrificed to image spleen, liver, kidney and lung.

Ellipsodial naAPCs demonstrated superior pharmacokinetic profiles compared to the spherical naAPCs. Live whole animal imaging analysis revealed that the ellipsoidal naAPCs remained in the periphery for longer periods of time, as evidenced by the greater signal distributed throughout the animal (compare Figure 4a and 4b). Images of the blood collected were analyzed by Image J to quantitatively examine the elimination from the blood over the first hour of the experiment. Results indicate that ellipsoidal naAPCs maintained a higher concentration in the bloodstream than spherical naAPCs, sustained over 40 min (Figure 4c). By fitting a first-order exponential decay curve we extracted the time constants for blood elimination and calculated the half-life. Ellipsodal naAPCs exhibited a significantly ($p < 0.05$) longer half-life at 34.8 min +/− 0.8 min than the spherical naAPCs at 25.2 min +/− 2.8 min (Figure 4d). In order to further characterize resistance to uptake by the RES, we quantified the signal obtained from the regions corresponding to the liver and spleen and subtracted it from the signal obtained from the entire animal. This value was then normalized to the signal measured over the entire region of the animal to obtain a parameter termed the dispersion fraction. The higher nanoellipsoidal circulation concentration was reflected in the dispersion fraction at the 1 hour time point (Figure 4e), further validating the

finding that the ellipsoidal naAPCs could resist RES uptake compared to spherical naAPCs. No significant difference was noted at the longer 2 hour and 4 hour timepoints, which was expected due to the particle half-lives. Spleen and liver accumulation of the naAPC was similar based on image analysis of the 1 hour, 2 hour, and 4 hour timepoints (Figure S4). Organ distribution analysis demonstrated similar endpoint distributions for the spherical and non-spherical naAPC (Figure S5).

Finally, given the advantages of the ellipsoidal aAPC compared to the spherical aAPC seen *in vitro*, including superior T-Cell stimulation, reduced non-specific cell uptake, and better half life/distribution upon systemic injection, we were interested to evaluate the *in vivo* T-Cell stimulatory capabilities of the ellipsoidal naAPC versus the spherical naAPC. To this end, we utilized an adoptive immunotherapy murine model. We irradiated Thy 1.2+ C57BL/6 mice with a sublethal dose of radiation and then administered the antigen specific aAPC and Thy 1.1+ PMEL T-cells simultaneously via intravenous tail vein injection. Mice received either the 2-fold stretched ellipsoidal aAPC with T-Cells, the spherical aAPC with T-Cells, or T-Cells alone. On days 6, 8, and 10 post injection, the mice were bled retroorbitally and the blood was analyzed for PMEL T-Cell expansion through the use of labeled anti-CD8 and anti-Thy 1.1 antibodies and flow cytometry. At the end of 10 days, the mice were sacrificed, and the spleen and lymph nodes were dissected and analyzed for PMEL T-Cell expansion.

Ellipsoidal naAPCs mediated significantly higher PMEL CD8+ T-Cell expansion *in vivo* compared to spherical naAPCs over the course of the experiment as evidenced by blood analysis of PMEL T-Cell content (Figure 5a). On both day 6 and day 8, there was a statistically significant increase in ellipsoidal aAPC mediated T-Cell expansion compared to both spherical mediated T-Cell expansion and no aAPC treatment. On day 10, there was a statistically significant increase of the ellipsoidal aAPC mediated expansion of PMEL T-Cells compared to control. However, the spherical naAPC could not mediate a statistically significant increase in T-Cell proliferation compared to the control groups on any of the days measured. The ellipsoidal aAPC induced nearly a 3-fold greater expansion over the no treatment group and a 2-fold greater expansion over the spherical aAPC group. Analysis of the dissected spleen (Figure 5b) and lymph nodes (Figure 5c) supported the observations seen in the blood with an overall greater increase in PMEL T-Cell content of the ellipsoidal aAPC compared to the spherical aAPC and the no treatment groups. This difference was statistically significant between the ellipsoidal and no treatment groups only.

Nanoellipsoidal aAPCs offer multiple advantages over traditional spherical aAPCs. We demonstrated that, under the same synthesis conditions and particle surface protein content, non-spherical naAPCs are more effective at antigen specific induction of CTLs than spherical naAPCs. In addition, these non-spherical naAPCs demonstrated stronger *in vivo* stimulation of immune cells and enhanced pharmacokinetic properties. Previous studies of nano aAPCs focused on the use of quantum dots, spherical PLGA particles, and magnetic iron dextran particles.[7, 10, 33] We showed for the first time that the efficacy of biodegradable nanoscale aAPCs can be enhanced by modulating shape in synthesis. By utilizing a non-spherical biodegradable nanoparticle, ellipsoidal naAPCs achieved T-Cell activation and proliferation comparable to previously reported nano aAPCs at a reduced

overall protein dose.[7] In addition to offering an efficiency advantage, ellipsoidal nanoparticles offer reduced cellular uptake by macrophages and endothelial cells *in vitro* and resist hepatic and splenic elimination *in vivo*. Taken together, the enhanced immune stimulatory capabilities and systemic biodistribution of ellipsoidal naAPCs make them a promising platform for “off the shelf” immunotherapy and nanomedicine.

Supplementary Material

Refer to Web version on PubMed Central for supplementary material.

Acknowledgements

The authors thank the Johns Hopkins University - Wallace H. Coulter Translational Partnership, the NIH (R01-EB016721), and the Wilmer Core Grant, Imaging and Microscopy Core Module (P30-EY001865), for support of this research. The authors thank Jay Burns (Johns Hopkins Biomedical Engineering Machine Shop) and Randall S. Meyer for fabricating the particle stretchers. RAM thanks the NIH Cancer Nanotechnology Training Center (R25CA153952) at the JHU Institute for Nanobiotechnology for fellowship support. JCS and KP thank the NIH MSTP program for support. KP is supported in part by a Cancer Research Institute Predoctoral Fellowship.

References

1. Engelhard VH, Strominger JL, Mescher M, Burakoff S. Proc. Natl. Acad. Sci. U.S.A. 1978; 75:5688. [PubMed: 310125]
2. Giannoni F, Barnett J, Bi K, Samodal R, Lanza P, Marchese P, Billetta R, Vita R, Klein MR, Prakken B. J. Immunol. 2005; 174:3204. [PubMed: 15749850]
3. Ugel S, Zoso A, De Santo C, Li Y, Marigo I, Zanovello P, Scarselli E, Cipriani B, Oelke M, Schneck JP. Cancer Res. 2009; 69:9376. [PubMed: 19934317]
4. Oelke M, Maus MV, Didiano D, June CH, Mackensen A, Schneck JP. Nat. Med. 2003; 9:619. [PubMed: 12704385]
5. Levine BL, Bernstein WB, Connors M, Craighead N, Lindsten T, Thompson CB, June CH. J. Immunol. 1997; 159:5921. [PubMed: 9550389]
6. Maus MV, Riley JL, Kwok WW, Nepom GT, June CH. Clin. Immunol. 2003; 106:16. [PubMed: 12584046]
7. Perica K, De León Medero A, Durai M, Chiu YL, Bieler JG, Sibener L, Niemöller M, Assenmacher M, Richter A, Edidin M. Nanomed.-Nanotechnol. 2014; 10:119.
8. Mescher M. J. Immunol. 1992; 149:2402. [PubMed: 1527386]
9. Han H, Peng J-R, Chen P-C, Gong L, Qiao S-S, Wang W-Z, Cui Z-Q, Yu X, Wei Y-H, Leng X-S. Biochem. Biophys. 2011; 411:530.
10. Steenblock ER, Fahmy TM. Mol. Ther. 2008; 16:765. [PubMed: 18334990]
11. Steenblock ER, Fadel T, Labowsky M, Pober JS, Fahmy TM. J. Biol. Chem. 2011; 286:34883. [PubMed: 21849500]
12. Tao Z, Hong G, Shinji C, Chen C, Diao S, Antaris AL, Zhang B, Zou Y, Dai H. Angew. Chem. Int. Ed. 2013; 125:13240.
13. Gao X, Cui Y, Levenson RM, Chung LW, Nie S. Nat. Biotechnol. 2004; 22:969. [PubMed: 15258594]
14. Md S, Ali M, Baboota S, Sahni JK, Bhatnagar A, Ali J. Drug Dev. Ind. Pharm. 2013; 40:278. [PubMed: 23369094]
15. Choi HS, Liu W, Liu F, Nasr K, Misra P, Bawendi MG, Frangioni JV. Nat. Nanotechnol. 2009; 5:42. [PubMed: 19893516]
16. Ye F, Barrefelt Å, Asem H, Abedi-Valugerdi M, El-Serafi I, Saghafian M, Abu-Salah K, Alrokayan S, Muhammed M, Hassan M. Biomaterials. 2014; 35:3885. [PubMed: 24495486]
17. Toita R, Nakao K, Mahara A, Yamaoka T, Akashi M. Bioorgan. Med. Chem. 2013; 21:6608.

18. Liu J, Yu M, Zhou C, Zheng J. Mater. Today. 2013; 16:477.
19. Kulkarni SA, Feng S-S. Pharm. Res. 2013; 30:2512. [PubMed: 23314933]
20. Chou LY, Zagorovsky K, Chan WC. Nat. Nanotechnol. 2014
21. Merkel TJ, Herlihy KP, Nunes J, Orgel RM, Rolland JP, DeSimone JM. Langmuir. 2009; 26:13086. [PubMed: 20000620]
22. Glotzer SC, Solomon MJ. Nat. Mater. 2007; 6:557. [PubMed: 17667968]
23. Geng Y, Dalhaimer P, Cai S, Tsai R, Tewari M, Minko T, Discher DE. Nat. Nanotechnol. 2007; 2:249. [PubMed: 18654271]
24. Muro S, Garnacho C, Champion JA, Leferovich J, Gajewski C, Schuchman EH, Mitragotri S, Muzykantov VR. Mol. Ther. 2008; 16:1450. [PubMed: 18560419]
25. Adriani G, de Tullio MD, Ferrari M, Hussain F, Pascazio G, Liu X, Decuzzi P. Biomaterials. 2012; 33:5504. [PubMed: 22579236]
26. Florez L, Herrmann C, Cramer JM, Hauser CP, Koynov K, Landfester K, Crespy D, Mailander V. Small. 2012; 8:2222. [PubMed: 22528663]
27. Barua S, Yoo J-W, Kolhar P, Wakankar A, Gokarn YR, Mitragotri S. Proc. Natl. Acad. Sci. U.S.A. 2013; 110:3270. [PubMed: 23401509]
28. Sharma G, Valenta DT, Altman Y, Harvey S, Xie H, Mitragotri S, Smith JW. J. Control Release. 2010; 147:408. [PubMed: 20691741]
29. Kolhar P, Anselmo AC, Gupta V, Pant K, Prabhakarpandian B, Ruoslahti E, Mitragotri S. Proc. Natl. Acad. Sci. U. S. A. 2013; 110:10753. [PubMed: 23754411]
30. Sunshine JC, Perica K, Schneck JP, Green JJ. Biomaterials. 2014; 35:269. [PubMed: 24099710]
31. Ho C, Keller A, Odell J, Ottewill R. Colloid Polym. Sci. 1993; 271:469.
32. Champion JA, Katare YK, Mitragotri S. Proc. Natl. Acad. Sci. U. S. A. 2007; 104:11901. [PubMed: 17620615]
33. Perica K, Tu A, Ricter A, Bieler JG, Edidin M, Schneck JP. ACS Nano. 2014; 8:2252. [PubMed: 24564881]

Non-spherical nanodimensional artificial antigen presenting cells (naAPCs) offer the potential to systemically induce an effective antigen-specific immune response. In this report it is shown biodegradable ellipsoidal naAPCs mimic the T-Cell/APC interaction better than equivalent spherical naAPCs. In addition, it is demonstrated ellipsoidal naAPCs offer reduced non-specific cellular uptake and a superior pharmacokinetic profile compared to spherical naAPCs.

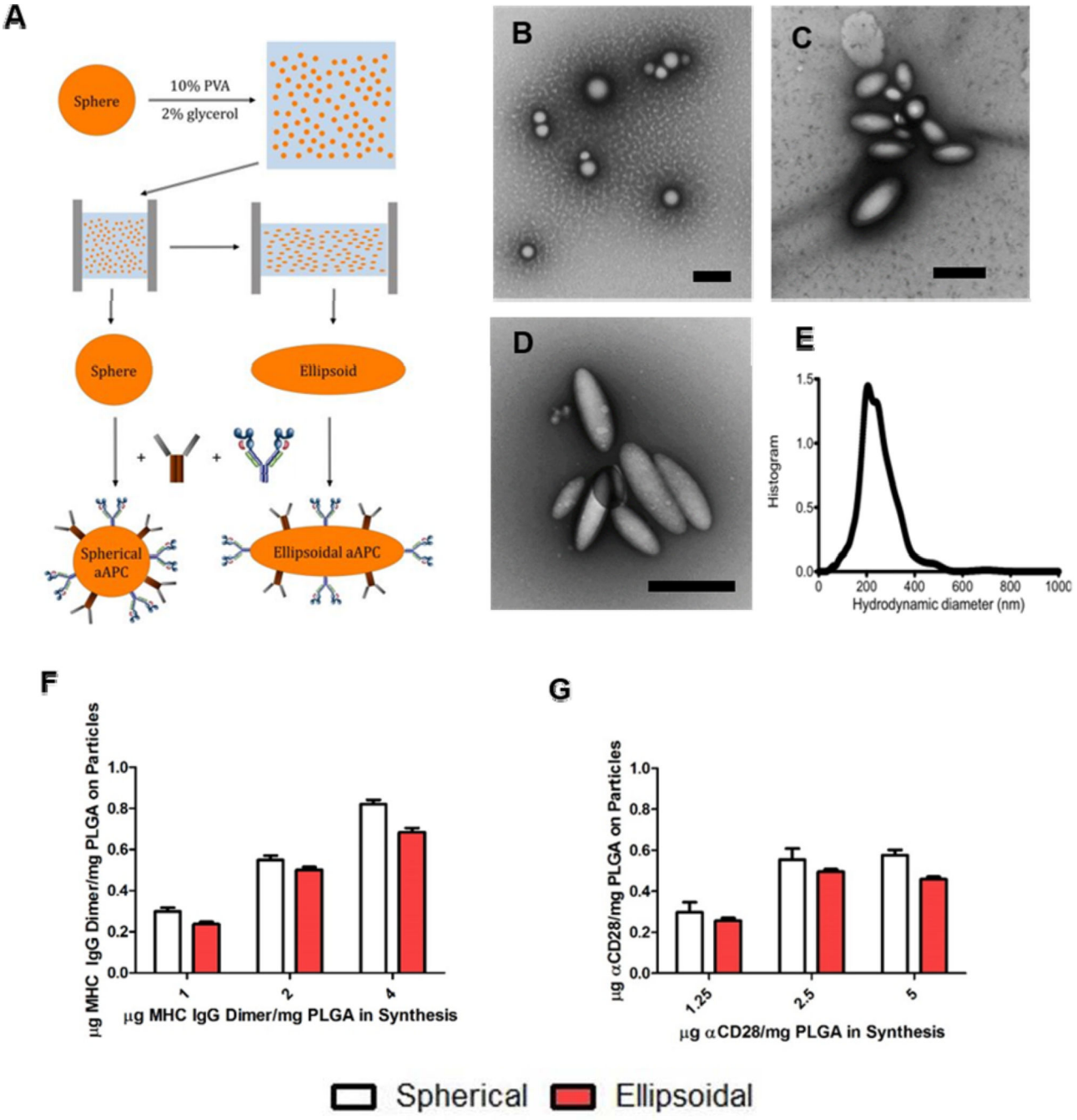

Figure 1.

Non-spherical and spherical nanodimensional artificial antigen presenting cell (naAPC) characterization. (a) PLGA nanoparticles were synthesized by single emulsion and elongated utilizing the film stretching method. Conjugation of MHC Db Ig Dimer and anti CD-28 mediated by EDC/NHS chemistry resulted in naAPCs. (b,c,d) TEM images of (b) non-stretched spherical particles (c) 2-fold stretched particles, and (d) 3-fold stretched particles. Scale bars are 500 nm. (e) Particles were sized by Nanoparticle Tracking Analysis and determined to be 224 nm in size. The particle protein conjugation efficiency on spherical

and 2-fold stretched ellipsoids for (f) MHC Db Ig dimer and (g) anti CD-28 was analyzed by conjugation of fluorescent protein. Conjugation results demonstrate similar amounts of protein bound to each particle shape. Error bars represent standard errors of >3 trials.

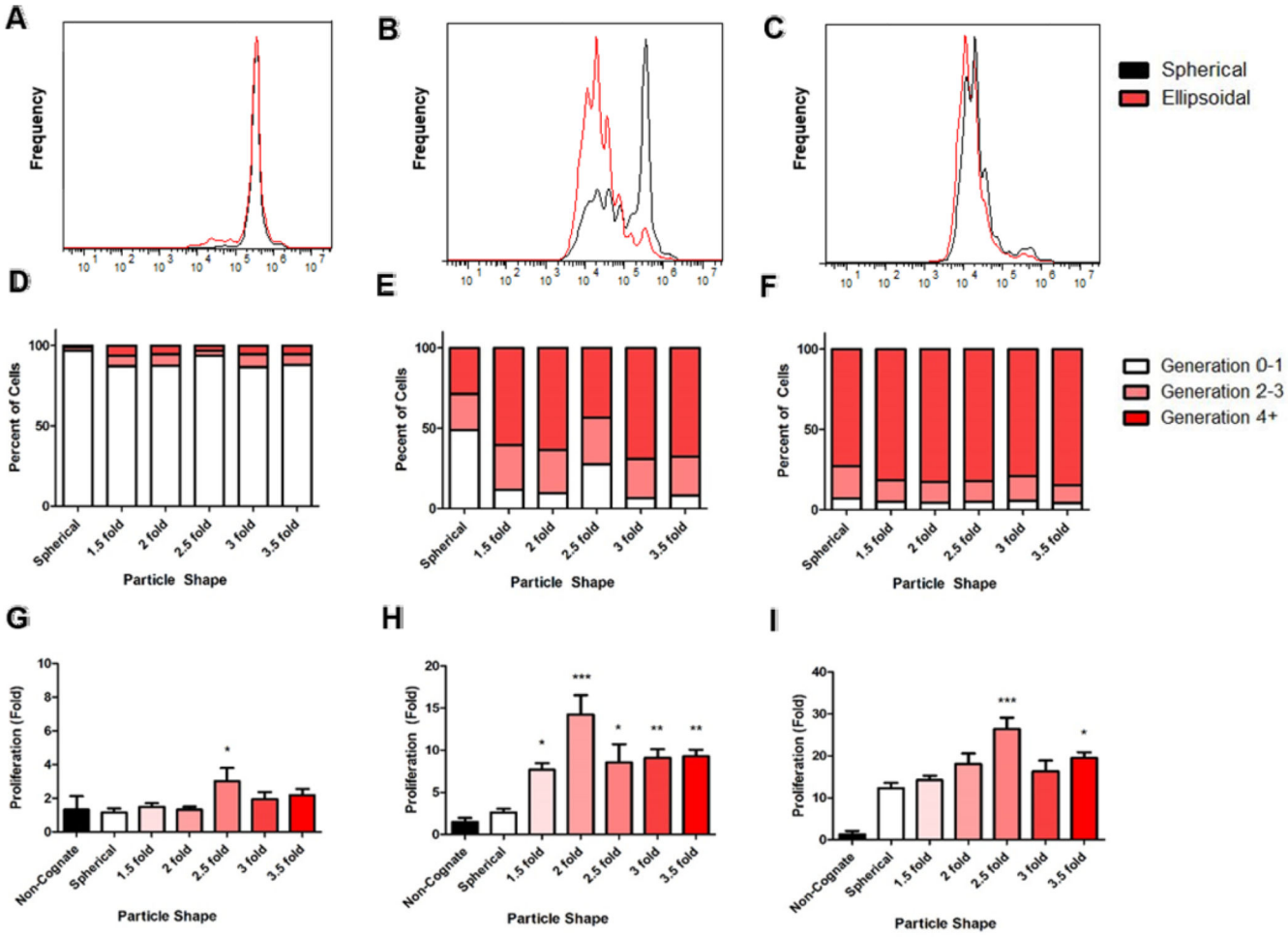

Figure 2.

Non-spherical naAPCs stimulate T-Cells more effectively than spherical naAPCs *in vitro*. PMEL transgenic CD8+ T-Cells were incubated with (a,d,g) 0.01 mg , (b,e,h) 0.1 mg, (c,f,g) 1 mg of spherical (black/white) and 2-fold stretched, ellipsoidal (red) naAPCs of various aspect ratios. Cells were stained with CFSE and evaluated by flow cytometry for proliferation after 3 days of incubation with aAPCs (a-c). Generation analysis of CFSE flow cytometry data demonstrates increased proliferation of cells in non-spherical aAPC groups (d-f). Cells were also evaluated after 7 days of incubation by manual counting and normalizing cell titers to an untreated condition (g-i). Results indicate ellipsoidal nanoparticles of higher aspect ratios stimulate CD8+ T-Cells more effectively than their spherical counterparts (* = $p < 0.05$, ** = $p < 0.01$, *** = $p < 0.001$ compared to spherical). Error bars represent standard errors > 3 replicates.

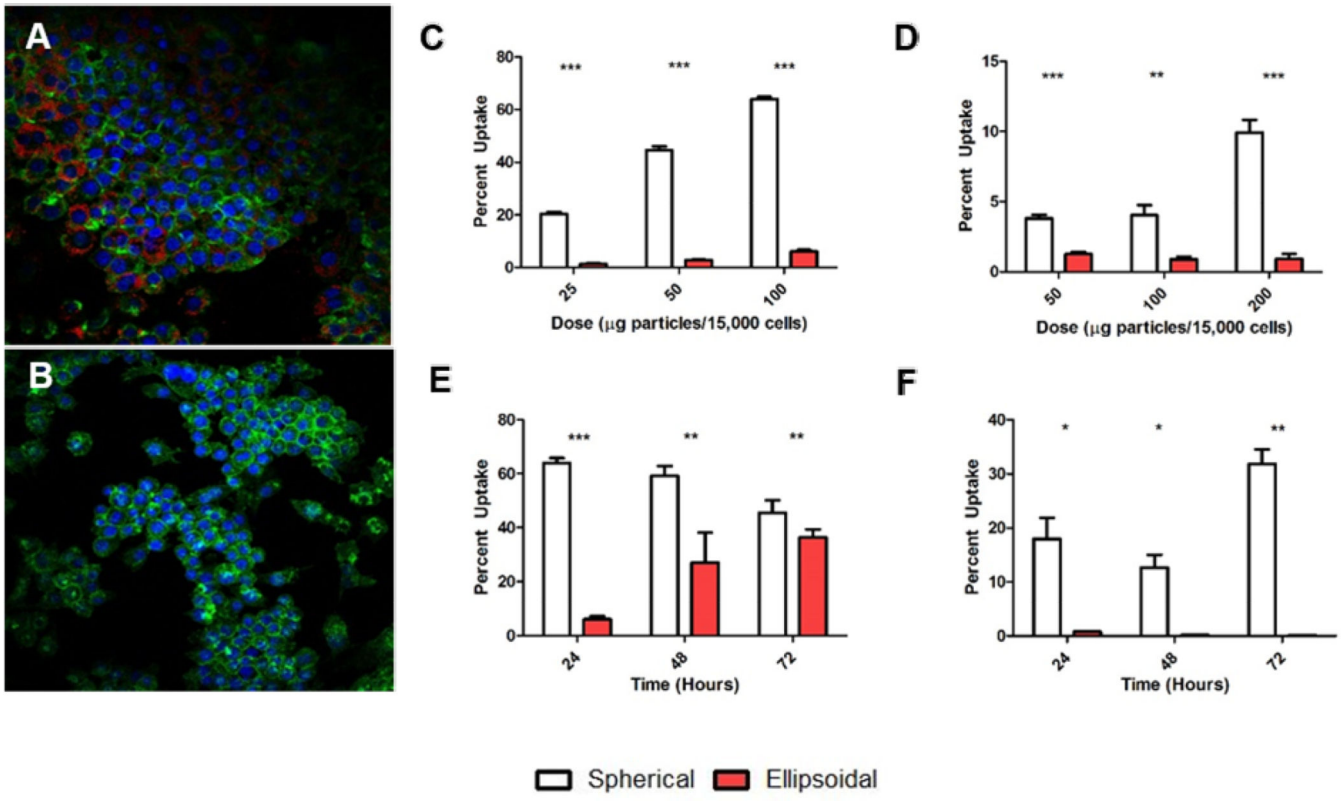

Figure 3.

Nanoparticle uptake is shape dependent. RAW macrophages were incubated with 0.5 mg (a) nanospherical and (b) 2-fold stretched nanoellipsoidal particles encapsulating TAMRA per 15,000 cells for 24 hours. Confocal micrographs show clear uptake of spherical particles compared to ellipsoidal aAPCs (Blue = DAPI, Green = Actin, Red = Particles). RAW macrophages were incubated with nanospherical and 2-fold stretched nanoellipsoidal particles at varying (c) doses or (e) times. Macrophages showed clear preference for spherical nanoparticle uptake which was maintained through 2 days and up to 200 μg/15,000 cells. Similar experiments were repeated with HUVECs with varying (d) dose and (f) time. Results indicate that HUVECs had near complete preference for spherical nanoparticles over 2-fold stretched ellipsoidal nanoparticles. Error bars represent standard error of the mean with n>3 for all experiments.

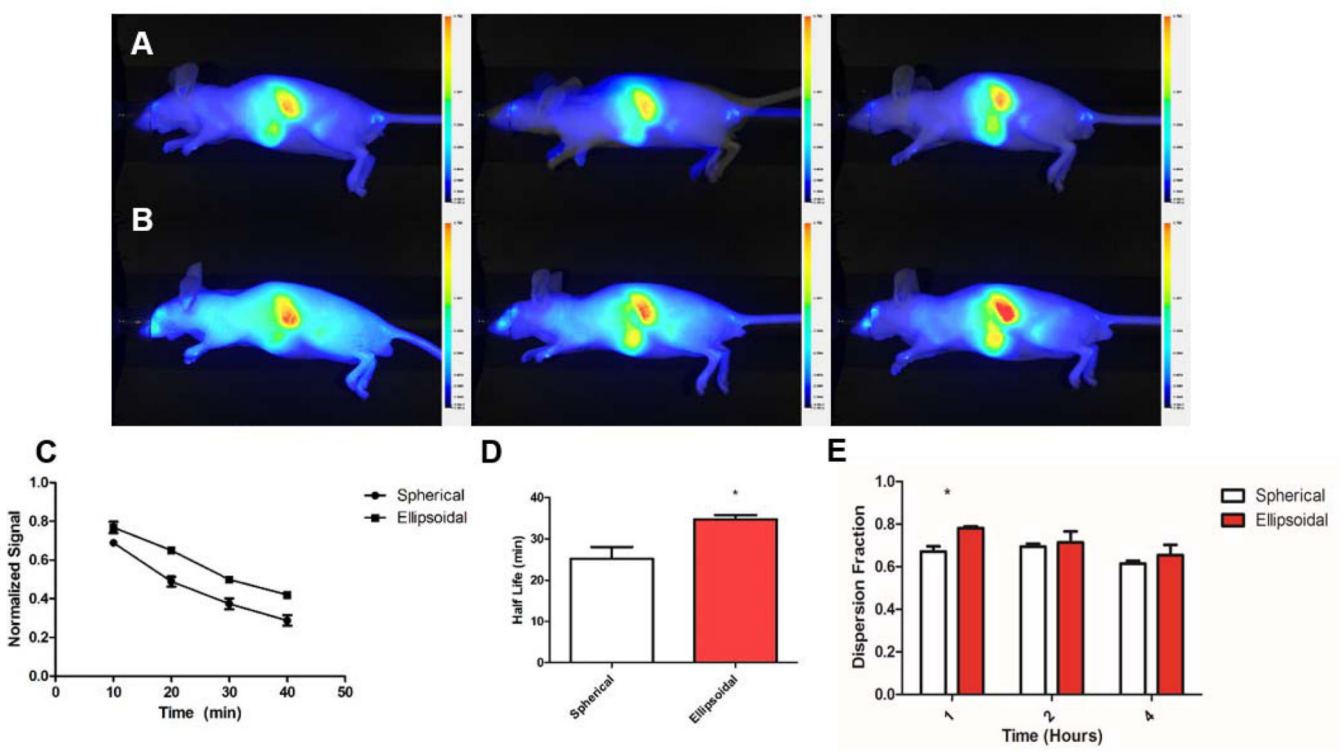

Figure 4.

Non-spherical nanoellipsoidal aAPCs have superior pharmacokinetics over nanospherical aAPCs. Conjugated (a) spherical and (b) 2-fold stretched ellipsoidal naAPC particles encapsulating a near IR fluorophore were injected intravenously into nude mice. Animals were imaged at 1 hour (left), 2 hours (middle), and 4 hours (right). (c) Blood collected retroorbitally at 10 min intervals was imaged and quantified for fluorescence over the first hour post injection. Results show the nanoellipsoidal aAPCs circulate at higher concentrations over the time periods examined, and (d) have a longer half-life (* = $p < 0.05$). (e) Two regions of interest from (a) and (b) were quantified: The entire animal, and the entire animal minus the region of the spleen and liver. The ratio of these values was computed to give the distribution throughout the animal. Nanoellipsoidal aAPCs demonstrated greater dispersion throughout the animal at the 1 hour time point (* = $p < 0.05$). Error bars represent standard error of the mean with n = 3 for all experiments.

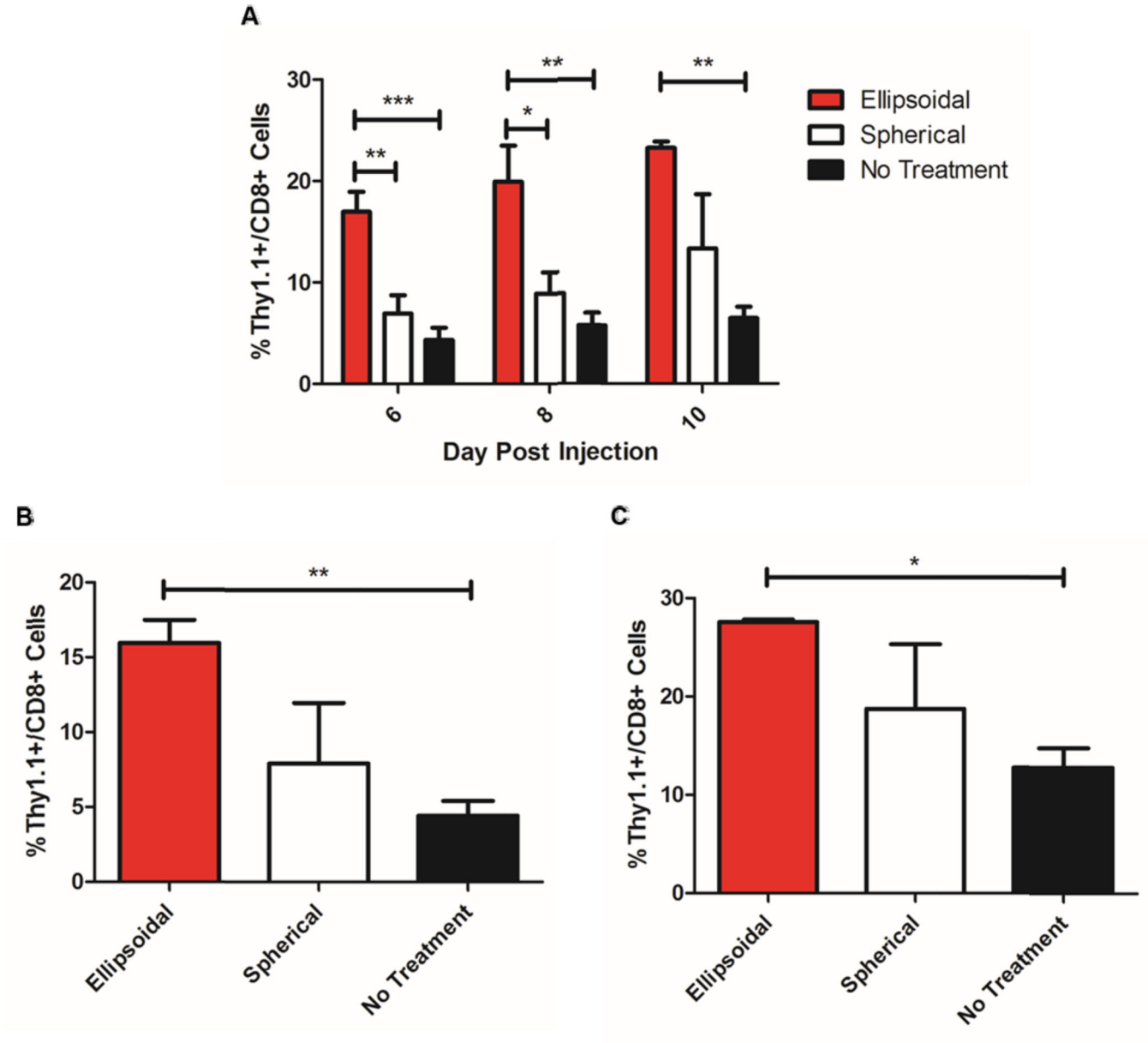

Figure 5.

2-fold stretched ellipsoidal nano aAPCs stimulate T-Cells superiorly to spherical nano aAPCs. Ellipsoidal and spherical aAPCs were injected intravenously into irradiated mice accompanied by 10^6 antigen specific CD8+ T-Cells bearing the marker Thy 1.1. "No treatment" groups received T-Cells only. (a) Blood was collected retroorbitally on day 6, 8, and 10 post injection and analyzed for the percent of CD8+ cells that were also Thy 1.1 positive. Results indicate a statistically significant increase in the percentage of antigen specific T-Cells stimulated *in vivo* by ellipsoidal aAPCs compared to spherical aAPCs on day 6 and 8 post injection and no aAPC control groups on all days analyzed. The mice were killed on day 10 post injection and the spleen and lymph nodes were dissected and analyzed for percent CD8+ cells that were also Thy 1.1 positive. Results show that for both (b) spleens and (c) lymph nodes, there was an increase in the Thy 1.1 positive cells in the

ellipsoidal groups compared to spherical, and statistically significant increase of ellipsoidal over no-treatment. Error bars indicate the SEM of n = 3 to 5 mice per group. (* = $p<0.05$, ** = $p<0.01$, *** = $p<0.001$).